Available online at www.sciencedirect.com
SCIENCE DIRECT®
Polymer 45 (2004) 1903–1911
polymer
www.elsevier.com/locate/polymer

Effect of chemical compositional distribution on solid-state structures and properties of poly(3-hydroxybutyrate-*co*-3-hydroxyvalerate)

Naoko Yoshie[a,*], Miwa Saito[b], Yoshio Inoue[b]

[a]*Institute of Industrial Science, University of Tokyo, Komaba 4-6-1, Meguro-ku, Tokyo 153-8505, Japan*
[b]*Department of Biomolecular Engineering, Tokyo Institute of Technology, 4259 Nagatsuta, Midori-ku, Yokohama 226-8501, Japan*

Received 22 October 2003; received in revised form 26 December 2003; accepted 17 January 2004

Abstract

Solid-state structures and crystallization kinetics were compared between poly(3-hydroxybutyrate-*co*-3-hydroxyvalerate) [PHB-HV] and PHB/PHB-HV blends exhibiting the cocrystallization. As cocrystallizable blends, both the blends showing complete cocrystallization, i.e. the PHB content in the crystalline phase is the same as that of the whole blends, and the blends forming a PHB-rich crystalline phase were used. The PHB and HV content in the cocrystalline phase were determined by high-resolution solid-state ^{13}C NMR spectroscopy. In order to determine these contents with a minimum experimental error, site-specific ^{13}C-labeled PHB/PHB-HV blends and PHB-HV copolymers were used. The crystallinity, lamellar structures, spherulite growth rate, and melting behavior were analyzed by wide-angle X-ray diffraction, small-angle X-ray scattering, polarized microscope, and differential scanning calorimetry, respectively. In these data, no difference was observed between the complete-cocrystallizable PHB/PHB-HV blends and the PHB-HV copolymers with the same overall HV content. On the other hand, the PHB/PHB-HV blends forming a PHB-rich crystalline phase has the amorphous layers thicker than that of the PHB-HV copolymers with the same overall HV content. Based on the collected data, the similarity and differences in the solid-state structures and properties between PHB-HV copolymers and cocrystallizable PHB/PHB-HV blends were discussed.

Keywords: Bacterial copolyester; Chemical composition distribution; Cocrystallization

1. Introduction

Bacterially synthesized poly(hydroxyalkanoate)s [PHAs] attract much attention because they can be produced from varied renewable resources and are truly biodegradable and highly biocompatible thermoplastic materials. Therefore, PHAs are expected to contribute to the construction of environmentally sustainable society. The most representative member of this family is poly(3-hydroxybutyrate) [PHB], which is a semi-crystalline material with a fairly high melting temperature about 170 °C. PHB degrades to crotonic acid at temperatures of only a few degrees above the melting temperature. The unstable nature in the melt, along with brittleness, of PHB limits its range of application fields. Biosynthesis of copolymers containing hydroxyalkanoate units other than HB is a valuable approach to overcome the shortcomings of PHB and to diversify the physical and mechanical properties of PHA materials. Biosynthesis and characterization of various copolymers, including copolymers of HB with 3-hydroxyvalerate (HV) [1,2], 3-hydroxypropionate (HP) [3], 3-hydroxyhexanoate (3HH) [4], and 4-hydroxybutyrate (4HB) [5], have been reported.

In general, bacterial PHB-based copolymers have very broad and/or polymodal distribution of chemical composition [6]. Properties of copolymers depend not only on the average chemical composition but also on its distribution. Therefore, researchers on the practical applications of PHB-based copolymers require preliminary knowledge of the influences of the average composition and its distribution on various properties. From this point of view, the compositional fractionation of PHB-based copolymers and the characterizations of both the original copolymers and their fractions were reported [7–12]. The influences of the broad composition distribution on crystallization behavior, the resultant solid-state structure, and physical properties

* Corresponding author. Address: Institute of Industrial Science, University of Tokyo, Komaba 4-6-1, Meguro-ku, Tokyo 153-8505, Japan. Tel.: +81-3-5452-6309; fax: +81-3-5452-6311.
E-mail address: yoshie@iis.u-tokyo.ac.jp (N. Yoshie).

0032-3861/$ - see front matter © 2004 Elsevier Ltd. All rights reserved.
doi:10.1016/j.polymer.2004.01.025

including biodegradation behavior were clearly demonstrated.

The relation between the composition distribution and various properties were further investigated through the analysis of the blends of PHB with fractionated PHB-based copolymers [13–16]. These blends are regarded as a PHB-based copolymer with bimodal composition distribution. Such blends show wide variety of phase structures depending on the chemical structure and the composition of the copolymers. For the case of the blends of PHB and PHB-HV, observable phase structures include cocrystallization of PHB and PHB-HV, coexistence of two or more crystalline phases formed by phase segregation upon the crystallization, and immiscible phase separation, which changes in this order with the increase of the HV content of PHB-HV [13,15–19]. In a previous paper [14], we have shown the cocrystals of the blends further classified into two types, i.e. PHB-rich crystals and complete cocrystals where PHB content is the same as the blend composition, through the analysis of the PHB content in the crystalline phase by ^{13}C cross-polarization magic-angle sample spinning (CPMAS) NMR spectroscopy. In order to make contrast between PHB and PHB-HV, the samples used in that analysis was the blends of normal PHB-HV with PHB of which methylene carbon was selectively labeled by ^{13}C.

Then, one of the remaining problems is where is the boundary between the blend that can be regarded as a simple copolymer practically and the blend that must be treated as an exact blend. Can we regard a cocrystallizable PHB/PHB-HV blend as a simple PHB-HV copolymer? In order to answer this question, we compare the solid-state structures and the crystallization kinetics between PHB-HV copolymers and cocrystallizable PHB/PHB-HV blends in this study. As structural parameters, the composition in the cocrystalline phase, degree of crystallinity, long period and lamella thickness are analyzed. As will be described later, the complete description of the composition in the crystalline phase needs the HV content, in addition to the PHB content, in the crystalline phase. These two contents in the crystalline phase are determined by ^{13}C CPMAS NMR analysis of the blends of ^{13}C-labeled PHB and ^{13}C-labeled PHB-HV. The other parameters are estimated from the analyses of wide-angle X-ray diffraction (WAXD), differential scanning calorimetry (DSC), small-angle X-ray scattering (SAXS), and polarized microscopy.

2. Experimental section

2.1. Materials

Samples of PHB and PHB-HV were prepared by fermentation of *Ralstonia eutropha* H16 (ATCC17699) as previously reported [20]. Acetic acid was used as a carbon source for PHB preparation. ^{13}C-labeled PHB samples were produced from [2–4 mol% 2-^{13}C] acetic acid. When [*x* mol% 2-^{13}C] acetic acid is used as a carbon source, *x* mol% of the methyl and methylene carbons of PHB are selectively labeled with ^{13}C [20]. The carbon sources used for PHB-HV accumulation were mixtures of acetic and propionic acids. ^{13}C-labeled PHB-HV copolymers were produced from mixtures of natural acetic acid and [≈10 mol% 1-^{13}C] propionic acid. When a carbon source containing [*x* mol% 1-^{13}C] propionate is used, *x* mol% of the methine carbons of HV units is selectively labeled with ^{13}C [20]. When we need to discriminate the PHB [PHB-HV] samples with and without ^{13}C label explicitly, we denote them as PHB^{E} [PHB-HV^{E}] and PHB^{N} [PHB-HV^{N}], respectively. The PHB-HV samples isolated from bacteria were subjected to the compositional fractionation by using chloroform/heptane mixed solvent [7]. Three PHB-HV^{N} fractions (HV content 9, 15, and 21 mol%) and two PHB-HV^{E} fractions (HV content 6 and 13 mol%), in addition to three PHB^{E}, were used in this study.

Molecular characteristics of the PHB and PHB-HV samples are listed in Table 1. Molecular weights, HV contents, and ^{13}C contents of the labeled sites were determined by GPC, solution-state ^{1}H NMR spectroscopy, and solution-state ^{1}H-coupled ^{13}C NMR spectroscopy, respectively, as previously reported [14,21]. From the ^{13}C content of the labeled site, the ^{13}C content among all carbon atoms is calculated to be only ≈2 mol% for the labeled samples. This value is comparable to the natural abundance (1.1 mol%). Thus, we have assumed that the ^{13}C enrichment has no effect on the physical properties of the PHB^{E} and PHB-HV^{E} samples.

Blending of PHB and PHB-HV was performed by a conventional solvent-casting technique from chloroform solution using a glass Petri dish as a cast surface. Two blends of PHB^{E} and PHB-HV^{E}, i.e. PHB^{E}-3/PHB-6%HV^{E} and PHB^{E}-3/PHB-13%HV^{E}, were newly prepared for this study. Full analysis was performed for these samples. In order to improve the quality of discussion, the SAXS and WAXD analyses were also performed for PHB^{E}-1/PHB-9%HV^{N}, and PHB^{E}-2/PHB-15%HV^{N}. These two blends are the same sample used in the previous study [14], where the phase structure and the PHB content in the crystalline phase were determined by DSC and ^{13}C CPMAS NMR spectroscopy.

The analysis was made on the melt-crystallized films of PHB/PHB-HV blends and PHB-HV copolymers. The melt-crystallized films were prepared by compression molding performed on a Toyoseiki Mini Test Press-10. The cast films were inserted between aluminum plates with an aluminum spacer (0.1 mm thickness) and were compression-molded at 195 °C for 3 min under a pressure of 5 MPa. The molten samples were then cooled to 90 °C and kept for four weeks to reach the equilibrium crystallinity prior to the analysis.

2.2. Analytical methods

^{13}C CPMAS NMR spectra were recorded at 100 MHz on

Table 1
Molecular characteristics of PHB and PHB-HV

Polyester[a]	HV content[b] (%)	$M_w \times 10^{-5}$[c]	M_w/M_n[c]	^{13}C content (%)[d]	
				HB methylene	HV methine
PHB^E-1	0	10.9	2.0	2.7	1.1[e]
PHB^E-2	0	4.3	2.3	2.4	1.1[e]
PHB^E-3	0	6.0	2.4	3.4	1.1[e]
PHB-6%HV^E	5.9	7.9	2.4	1.1[e]	11.9
PHB-9%HV^N	9.2	7.2	2.7	1.1[e]	1.1[e]
PHB-13%HV^E	12.9	4.4	2.7	1.1[e]	11.7
PHB-15%HV^N	15.1	4.6	1.5	1.1[e]	1.1[e]
PHB-21%HV^N	21.0	7.1	2.3	1.1[e]	1.1[e]

[a] Superscript E and N indicate the samples with and without ^{13}C enrichment, respectively.
[b] Measured by ^1H NMR.
[c] Measured by GPC.
[d] Measured by ^1H-coupled ^{13}C NMR.
[e] Natural abundance of ^{13}C.

a VARIAN UNITY-400 NMR spectrometer equipped with CPMAS accessories. Spectra were acquired with a 5 s pulse repetition, a 50 kHz spectral width, 4 K data points, and 1200–4096 accumulations under high-power ^1H decoupling. Contact time and MAS rate were 2 ms and 4.0–6.0 kHz, respectively.

WAXD and SAXS measurements were made on a Rigaku RU-200 operated at 50 kV and 180 mA. Nickel-filtered Cu Kα radiation ($\lambda = 0.154$ nm) was used. WAXD patterns were recorded in the 2θ range 5–50° at a scan speed of 1.0 °/min at room temperature. Assuming that the diffraction peak from a crystallographic plane and the amorphous halo could be reproduced by a Gaussian curve and a sum of two Gaussian curves, respectively, diffraction patterns in the 2θ range 5–33° were resolved into a series of Gaussian peaks by curve fitting using damped least-squares algorithm. The degree of crystallinity (χ_{waxd}) was calculated from the relative areas of the resolved peaks. SAXS patterns were recorded in the 2θ range 0.1–2.5°. Each step increased 2θ by 0.004° and X-rays were collected for 4 s at each step. The first-order correlation function was estimated by applying an inverse Fourier transform to the scattering profile corrected by thermal background subtraction, extrapolation to $s = 0$ by Guinier's law and extrapolation to $s = \infty$ by Porod's law. The long period, L, of the samples was determined from the maximum of the first-order correlation function estimated from the SAXS patterns [22]. Assuming a simple two-phase model of lamellar morphology, lamellar thickness, L_c, can be estimated by the product of L and the volume fraction of crystallinity, χ_v. Since the difference between χ_v and χ_{waxd} is very small [21], we have estimated lamellar thickness, L_c, as a product of L and χ_{waxd}.

Thermal characterization was conducted on a SEIKO EXSTAR6000 system equipped with a DSC 220U. Melt-crystallized films of 3–6 mg were encapsulated in aluminum pans, and heated from room temperature to 200 °C at a heating rate of 20 °C/min. The melting temperature was taken as the peak top.

Spherulite growth rates were measured by polarized microscopy. Analysis was carried out with an Olympus BX 90 polarized microscope equipped with a Mettler FP82HT hot stage. Film samples were heated to 195 °C, kept at this temperature for 1 min and then cooled to 90 °C where the growth of spherulites was observed. The spherulite growth rate was taken as the slope of the plot of spherulite radius vs. time.

3. Results and discussion

3.1. Determination of composition in the crystalline phase of PHB^E/PHB-HV^E blends

3.1.1. DSC analysis

Fig. 1 shows the DSC melting thermograms of PHB^E-3/

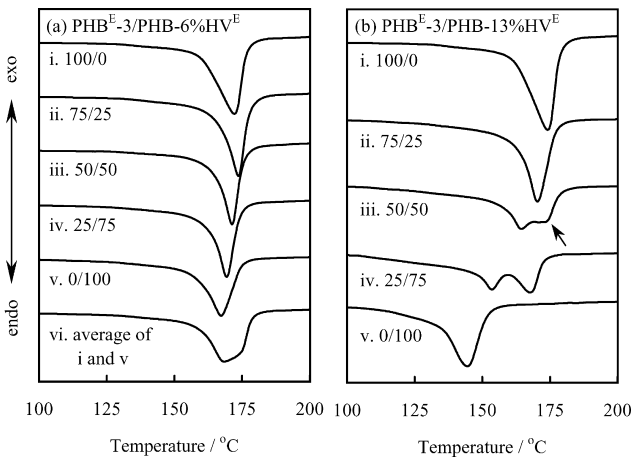

Fig. 1. DSC melting thermograms of PHB^E-3/PHB-6%HV^E (a) and PHB^E-3/PHB-13%HV^E (b). Calculated average curve (a-vi) of pure PHB^E-3 and PHB-6%HV^E is also shown. The arrow indicates the peak arising from recrystallization.

PHB-6%HV^{E} and PHB^{E}-3/PHB-13%HV^{E} blends. For PHB^{E}-3/PHB-6%HV^{E} blends, a single melting peak is observed. The proximity of the melting temperatures of PHB^{E}-3 and PHB-6%HV^{E} implies that the single peak behavior of the blends is just a result of overlapping of two melting peaks. This possibility is, however, denied by the calculated average curve of the thermograms of pure PHB^{E}-3 and PHB-6%HV^{E} shown in the figure. The thermogram for 50/50 PHB^{E}-3/PHB-6%HV^{E} blend is obviously different from the average curve. The peak of the former is much narrower than the latter. Therefore, we can confirm that only one crystalline phase is formed in PHB^{E}-3/PHB-6%HV^{E}.

For PHB^{E}-3/PHB-13%HV^{E}, the thermograms of 100/0, 75/25 and 0/100 blends show single melting peak while those of 50/50 and 25/75 blends show two peaks. When interpreting multiple melting peaks of a polymeric material, we must distinguish between peaks arising from phase-separated crystals and ones arising from crystals rearranged during heating run in the DSC apparatus. The distinction can be easily made by their response to variations in heating rate [23]. For the 50/50 PHB^{E}-3/PHB-13%HV^{E} blend, the relative intensity of the higher temperature peak decreased as the heating rate increased, indicating that this peak is ascribed to the melt/recrystallization process (data not shown). Only the lower temperature peak corresponds to the melting of the crystals formed at the crystallization temperature (90 °C). For the 25/75 blend, on the other hand, the variation of heating rate gave little effect on the relative intensity of the peaks. Therefore, two crystalline phases are formed in this blend at the crystallization temperature.

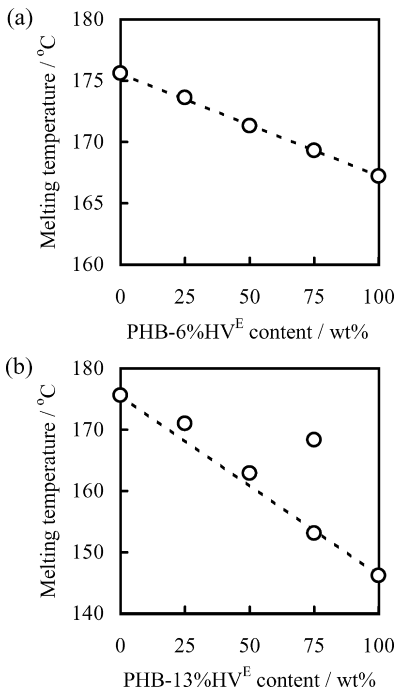

Fig. 2. Melting temperature of PHB^{E}-3/PHB-6%HV^{E} (a) and PHB^{E}-3/PHB-13%HV^{E} (b) as a function of blend composition.

Parts a and b of Fig. 2, respectively, shows the melting temperature of PHB^{E}-3/PHB-6%HV^{E} and PHB^{E}-3/PHB-13%HV^{E} blends as a function of weight fraction of the copolymers. Note that the peak ascribed to the melt/recrystallization is not plotted in this figure. The data for PHB^{E}-3/PHB-6%HV^{E} blends follow a straight line, suggesting that the PHB content in the crystalline phase is similar to the blend composition, i.e. complete cocrystallization occurs in these blends. For 75/25 and 50/50 PHB^{E}-3/PHB-13%HV^{E} blends, the data also suggest the complete cocrystallization. For 25/75 PHB^{E}-3/PHB-13%HV^{E}, the higher melting temperature is as high as that of PHB^{E}-3 while the lower one is between those of PHB^{E}-3 and PHB-13%HV^{E}. Therefore, the peaks are probably due to the melting of the PHB-rich crystals and of complete cocrystals, respectively.

The data of melting temperature only allow the estimation of the composition in the crystalline phase with limited accuracy because of the dependence of melting temperature on lamellar thickness. More precise estimation was done for PHB^{E}-3/PHB-6%HV^{E}, and PHB^{E}-3/PHB-13%HV^{E} blend by ^{13}C CPMAS NMR spectroscopy.

3.1.2. ^{13}C CPMAS NMR analysis

PHB-HV is known as a copolymer exhibiting isodimorphism, i.e. the cocrystallization of HB and HV units both in the PHB and PHV crystalline lattices [24,25]. However, the composition in the crystalline phase would not necessarily be the same as the HV content of the whole PHB-HV copolymer and actually changes with the crystallization condition [26,27]. The cocrystalline phase of PHB/PHB-HV is, therefore, composed of HB units from PHB, HB units from PHB-HV, and HV units from PHB-HV. The amount of HV unit in the cocrystalline phase is not the same as the product of the PHB-HV content in this phase and the HV content of the whole PHB-HV copolymer. Further, the composition in the crystalline phase probably changes depending on the blend composition and the crystallization condition. Therefore, the complete description of the phase structure of PHB/PHB-HV blends needs both the HV and PHB contents in the crystalline phase.

In a ^{13}C CPMAS NMR spectrum of PHB/PHB-HV, the peaks from PHB completely overlap with those from HB units of PHB-HV. The determination of the PHB content in the crystalline phase is impossible for the normal PHB^{N}/PHB-HV^{N} blend samples. Therefore, the contrast between PHB and PHB-HV was made by ^{13}C-labeling of methylene carbons of PHB (PHB^{E}-3) in this study. Further, when the total HV content in a PHB/PHB-HV blend is small, the resonances from HV units in the ^{13}C CPMAS NMR spectrum are so weak that the estimation of the relative peak area of them yields a large margin of experimental error. Thus, the methine resonance of HV units was enlarged by ^{13}C labeling for PHB-HV samples (PHB-6%HV^{E} and PHB-13%HV^{E}).

Fig. 3 shows ^{13}C CPMAS NMR spectra of PHB^{E}-3, 50/

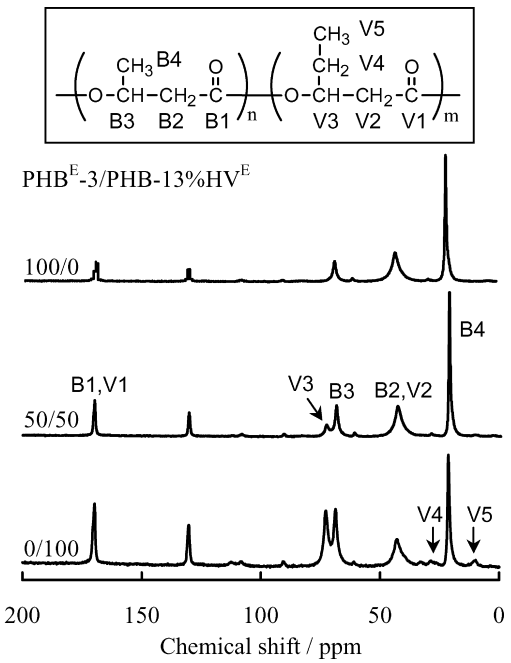

Fig. 3. 100 MHz ^{13}C CPMAS NMR spectra of PHB^{E}-3, 50/50 PHB^{E}-3/PHB-13%HV^{E}, and PHB-13%HV^{E}.

50 PHB^{E}-3/PHB-13%HV^{E}, and PHB-13%HV^{E}. Assuming a two-phase model, the main-chain methylene (B2, V2) and the methine (B3, V3) resonances of the samples are decomposed into the crystalline and amorphous peaks by curve fitting software using damped least-squares algorithm. Fig. 4 shows experimental and calculated spectra for the methine and methylene carbons of 50/50 PHB^{E}-3/PHB-13%HV^{E}. Since the resonance from crystalline V2 units is too weak to be resolved by curve fitting, the methylene (B2 + V2) resonance of the blends was decomposed into three Lorenzian curves, which are assigned to crystalline HB, amorphous HB, and crystalline + amorphous HV. Owing to the ^{13}C labeling, the methine (B3 + V3) resonance could be decomposed into four Lorenzian curves, which are assigned to crystalline HB, amorphous HB, crystalline HV, and amorphous HV. The assignment of these peaks was clearly described elsewhere [14,25,28]. The results of curve fitting for the blends are summarized in Table 2.

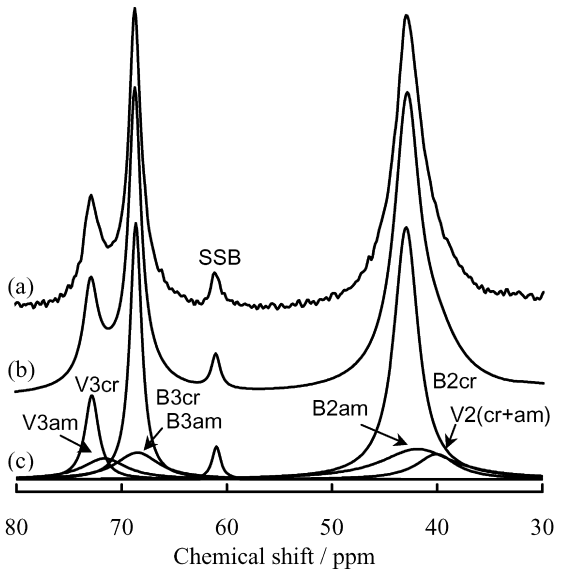

Fig. 4. Result of curve decomposition for methylene and methine resonances in 100 MHz ^{13}C CPMAS NMR spectra of 50/50 PHB^{E}-3/PHB-13%HV^{E}: (a) observed spectrum, (b) sum of curves in part c, (c) simulated curves.

The peak areas of the crystalline resonances from B2, B3 and V3 for PHB^{E}/PHB-HV^{E} blends are given by

$$A_{B2} = kr^{h}_{B2}f^{h}_{B2}P^{h}_{B} + kr^{c}_{B2}f^{c}_{B2}P^{c}_{B} \quad (1)$$

$$A_{B3} = kr^{h}_{B3}f^{h}_{B3}P^{h}_{B} + kr^{c}_{B3}f^{c}_{B3}P^{c}_{B} \quad (2)$$

$$A_{V3} = kr^{c}_{V3}f^{c}_{V3}P^{c}_{V} \quad (3)$$

where k is a constant: A, r, and f are peak area, ^{13}C population, and CP efficiency, respectively: superscripts c and h indicate copolymer (PHB-HV^{E}) and homopolymer (PHB^{E}) in the blend, respectively: subscripts B2, B3 and V3 identify the carbon site: P^{j}_{i} is a content of i unit from copolymer (j = c) or homopolymer (j = h) in the crystalline phase. From the definition, $P^{h}_{B} + P^{c}_{B} + P^{c}_{V} = 1$. In the present case, we can assume that $f^{h}_{B2} = f^{c}_{B2} = f_2$ and $f^{h}_{B3} = f^{c}_{B3} = f^{c}_{V3} = f_3$ because the chemical structure of HB unit is very similar to that of HV unit and the motions of the backbone methine and methylene carbons are extremely restricted in the crystalline region of both the copolymer and homopolymer. Since the B2 and B3 carbons in PHB-HV^{E} and the B3 carbon in PHB^{E} are not labeled, $r^{c}_{B2} = r^{c}_{B3} = r^{h}_{B3} = r_n$ (^{13}C natural abundance) ≈ 0.011. Then, the HV content in the crystalline phase P^{c}_{V} can be estimated from Eqs. (2) and (3) as

$$P^{c}_{V} = A_{V3}/(A_{B3}r^{c}_{V3}/r_n + A_{V3}) \quad (4)$$

The ratio of A_{B2} to A_{B3} is given by

$$R = A_{B2}/A_{B3} = f_2(P^{h}_{B}r^{h}_{B2}/r_n + P^{c}_{B})/f_3(P^{h}_{B} + P^{c}_{B}) \quad (5)$$

Considering that $P^{c}_{B} = P^{c}_{V} = 0$ for pure PHB^{E} and $P^{h}_{B} = 0$ for pure PHB-HV^{E}, we can determine the PHB content in the crystalline phase of PHB^{E}/PHB-HV^{E} by the comparison of the relative peak area of the blend, R^{blend}, with those of PHB^{E}, R^{PHB}, and PHB-HV^{E}, $R^{PHB\text{-}HV}$, as follows:

$$P^{h}_{B} = (1 - P^{c}_{V})[R^{PHB\text{-}HV} - R^{blend}]/(R^{PHB\text{-}HV} - R^{PHB}) \quad (6)$$

If r^{h}_{B2} was set to be much larger than the natural abundance, R^{PHB} and R^{blend} would be much larger than one and give relatively large experimental error in P^{h}_{B}. In order to minimize the error, r^{h}_{B2} of PHB^{E}-3 was set to be 3.4% in this study, resulting in the values of R^{PHB} and R^{blend} to be no more than 3.05. For the similar reason, r^{c}_{V3} of PHB-HV^{E} was set to be ca. 12%.

Table 2
Chemical shifts and peak areas of ^{13}C CPMAS NMR spectra for PHB^E/PHB-HV^E blends

	Chemical shift (ppm)							Relative peak area (%)							R^a
	B2[b]		V2	B3[b]		V3[b]		B2[b]		V2	B3[b]		V3[b]		
	Cr	am		cr	am	cr	am	cr	am		cr	am	cr	am	
PHB^E-3/PHB-6HV^E															
100/0	42.8	41.5		68.5	68.6			48.7	25.0		16.3	10.0			3.05
75/25	42.8	41.2		68.6	68.2	72.9	71.2	45.8	24.5	0.0	17.4	9.4	1.2	1.8	2.63
50/50	42.8	41.1	40.1	68.6	67.9	72.8	71.1	41.8	18.1	4.0	20.2	9.3	3.7	2.9	2.07
25/75	42.8	41.4	39.9	68.5	68.3	72.7	71.0	33.3	19.5	3.0	21.9	12.0	6.2	4.1	1.52
0/100	42.9	42.0	39.7	68.6	68.4	72.7	71.7	28.1	14.2	4.1	24.9	13.4	8.7	6.6	1.13
PHB^E-3/PHB-13%HV^E															
100/0	42.8	41.5		68.5	68.6			48.7	25.0		16.3	10.0			3.05
75/25	42.8	41.6	40.3	68.6	68.7	72.8	72.0	43.6	20.9	3.7	17.2	8.2	3.1	3.3	2.54
50/50	42.9	41.9	40.1	68.6	69.5	72.8	71.6	39.4	14.0	6.5	19.2	7.4	7.4	5.9	2.05
25/75	42.9	41.6	40.2	68.6	68.0	72.8	72.0	27.7	13.6	5.8	18.4	11.2	11.8	11.6	1.51
0/100	42.9	41.9	39.5	68.6	67.6	72.7	71.8	18.5	14.2	3.1	20.0	8.7	20.7	14.8	0.92

[a] R indicates the ratio of the peak areas for the crystalline B2 and crystalline B3 resonances.
[b] cr and am indicate crystalline and amorphous components, respectively.

3.1.3. Composition in the crystalline phase of PHB^E/PHB-HV^E blends

Fig. 5 shows the relation between the PHB content in the crystalline phases, P_B^h, and the blend composition for PHB^E-3/PHB-6%HV^E and PHB^E-3/PHB-13%HV^E blends crystallized at 90 °C. The data for 25/75 PHB^E-3/PHB-13%HV^E is excluded from the plot because the coexistence of the two crystalline phases in this blend complicates the interpretation. For these blends, the PHB content in the crystalline phase is similar to the whole composition, which indicates the occurrence of complete cocrystallization. PHB and PHB-HV chains are equally introduced into the crystalline phase without phase segregation and any other mechanism differentiating between PHB and PHB-HV. This result totally agrees with the suggestion of the DSC analysis.

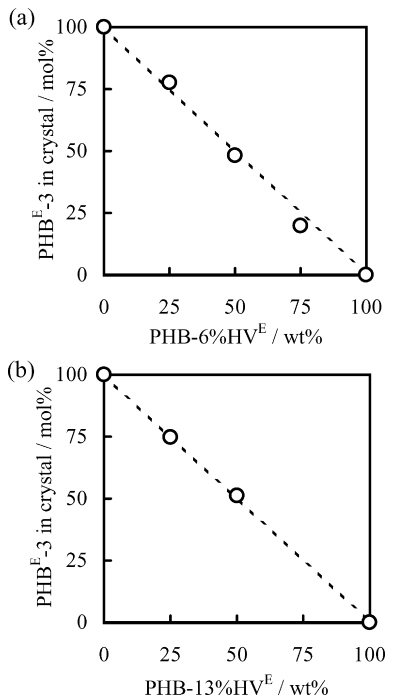

Fig. 5. PHB content in the crystalline phase of PHB^E-3/PHB-6%HV^E (a) and PHB^E-3/PHB-13%HV^E (b) as a function of blend composition. The broken line indicates the case in which both of the crystalline and amorphous phases have the same composition.

It has been shown in the previous paper [14] that cocrystallization also occurs in PHB^E-1/PHB-9%HV^N and PHB^E-2/PHB-15%HV^N. The degree of phase segregation is, however, different in these blends. The complete cocrystallization occurs in PHB^E-1/PHB-9%HV^N while PHB preferentially enters the crystalline phase of PHB^E-2/PHB-15%HV^N. The phase structures for the blends studied in this paper and in the previous paper are summarized in Table 3. For PHB/PHB-HV blends the extent of phase segregation during cocrystallization increases as the HV content of PHB-HV increases. The blends of PHB and PHB-HV containing 9 mol% or less HV exhibit complete cocrystallization, i.e. the PHB content in the crystalline phase is the same as the overall composition. When the HV content of PHB-HV increases to 15 mol%, phase segregation occurs

Table 3
Crystalline phases formed in PHB/PHB-HV blends

Blend	Crystalline phases[a]		
	75/25	50/50	25/75
PHB^E-3/PHB-6%HV^E	CC	CC	CC
PHB^E-1/PHB-9%HV^N	CC	CC	CC
PHB^E-3/PHB-13%HV^E	CC	CC	CC and BrC
PHB^E-2/PHB-15%HV^N	BrC	BrC	BrC

The data of PHBE-1/PHB-9%HVN and PHBE-2/PHB-15%HVN are cited from Ref. [14].
[a] CC and BrC indicate complete cocrystalline phase and PHB-rich cocrystalline phase, respectively.

with PHB crystallization and as a result, the PHB contents in the crystalline phase is higher than the overall PHB content. In PHB/PHB-13%HV, the complete-cocrystalline phase or the two separated crystalline phases are formed depending on the blend composition. When PHB is a minor component of the blend, both the PHB-rich crystals and complete cocrystals are formed.

The HV content in the crystalline phase is plotted against the HV content of the whole blend for PHB^{E}-3/PHB-6%HV^{E} and PHB^{E}-3/PHB-13%HV^{E} blends crystallized at 90 °C in Fig. 6. This figure indicates that the HV content in the crystalline phases is approximately one half of that in the whole blend for the complete cocrystallizable PHB/PHB-HV blends.

3.2. Comparison between cocrystallizable PHB/PHB-HV blends and PHB-HV copolymers

In Fig. 6, the HV content in the crystalline phases for PHB-HV copolymers containing 0–21 mol% HV are also plotted. For the PHB-HV copolymers containing less than 10 mol% HV, the ratio of the HV content in the crystalline phases to that of the whole copolymer is approximately one half, which is similar to the case of complete cocrystallizable PHB/PHB-HV blends. The coincidence in this ratio indicates the similarity in the structures inside the crystalline phase of the complete-cocrystallizable PHB/PHB-HV blends and PHB-HV copolymers.

It should be noted that the ratio for PHB-HV copolymers changes from one half to two third at 10 mol% HV [21]. This change was interpreted as an evidence of structural transition in the crystalline phase of PHB-HV copolymer. Though similar structural transition may occur in the cocrystallizable PHB/PHB-HV blends, this possibility cannot be discussed further because we could not prepare the blends containing more than 10% HV and still forming only complete-cocrystalline phase.

The comparison between PHB/PHB-HV blends and PHB-HV copolymers is continued through the X-ray and polarized microscope analysis. In addition to the blends studied in the previous sections, the blends of PHB^{E}-1/PHB-9%HV^{N} and PHB^{E}-2/PHB-15%HV^{N} are analyzed. The 25/75 PHB^{E}-3/PHB-13%HV^{E} is again excluded from the analysis.

Figs. 7–9, respectively, shows the degree of crystallinity estimated from WAXD patterns, the parameters of lamellar structure characterized by SAXS analysis, and the spherulite growth rate measured at 90 °C by polarized microscopy for cocrystallizable PHB/PHB-HV blends and PHB-HV copolymers as a function of HV content of the whole blend. The cocrystallizable blends are further categorized into two types; the one showing complete cocrystallization and the one forming PHB-rich crystals.

All the data for the complete-cocrystallizable PHB/PHB-HV blends shown in Figs. 6–9 exhibit the composition dependence similar to those of PHB-HV copolymers containing 10% HV or less. The coincidence in both the degree of crystallinity and the HV content in the crystalline phase indicates the similarity in the HV content in the amorphous phase. Since PHB and PHB-HV containing 25 mol% or less HV have been reported to be miscible [13], the structures in the amorphous phase of the complete cocrystallizable PHB/PHB-HV blends are practically the same as those of the PHB-HV copolymer of the same overall HV content. In addition to the HV content in the crystalline and amorphous phases, the data on spherulite growth rate, and lamellar structures of these blends are also similar to those of PHB-HV copolymers. Therefore, we can equate the complete-cocrystallizable PHB/PHB-HV blends with PHB-HV copolymers of the same overall HV content.

The situation for the blends forming PHB-rich crystals is little bit different. Fig. 8 shows that the long period of the PHB/PHB-HV blends forming PHB-rich crystalline phase is slightly longer than that of PHB-HV copolymers of the same overall HV content. Although the difference is very small,

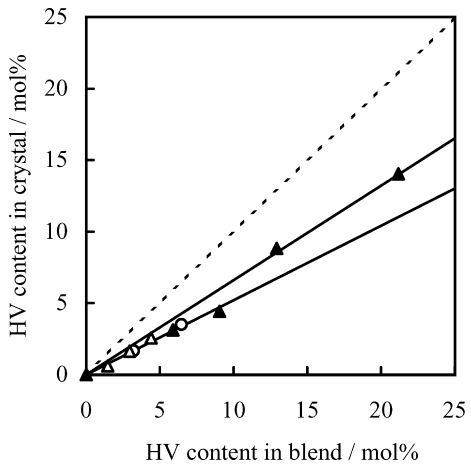

Fig. 6. HV content in the crystalline phase of PHB^{E}-3/PHB-6%HV^{E}(△) and PHB^{E}-3/PHB-13%HV^{E}(○) as a function of overall blend composition. The data for PHB-HV copolymers(▲) are also plotted. The broken line indicates the case where both the crystalline and amorphous phases have the same composition. The solid lines indicate the cases where the HV contents in the crystalline phase are one-half and two-thirds of the whole HV content.

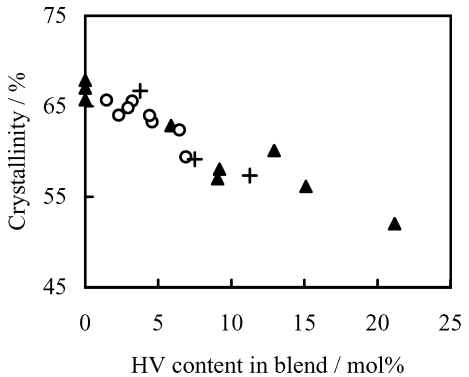

Fig. 7. Degree of crystallinity of PHB-HV copolymers (▲) and PHB/PHB-HV blends exhibiting complete-cocrystallization (○) and crystallization preferring PHB (+) as a function of overall HV content.

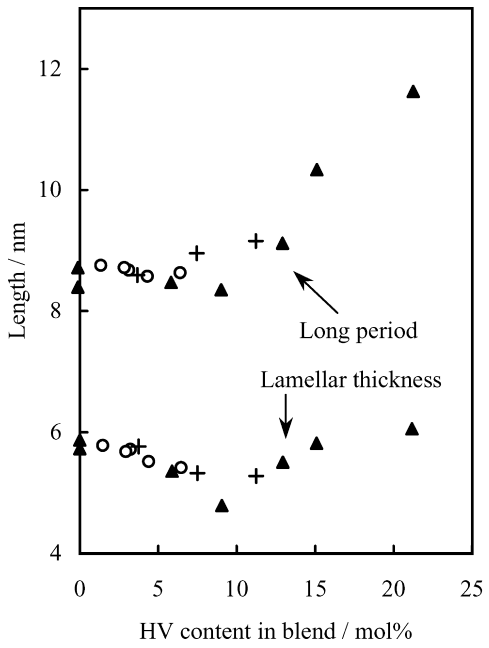

Fig. 8. Long period and lamellar thickness of PHB-HV copolymers (▲) and PHB/PHB-HV blends exhibiting complete-cocrystallization (○) and crystallization preferring PHB (+) as a function of overall HV content.

we believe that the difference is beyond the experimental error because repeated experiments show the similar results. On the other hand, the lamellar thickness of the blends forming PHB-rich crystalline phase is similar to that of the copolymers. This indicates that the blends have the amorphous layers thicker than the copolymers. Therefore, the composition in the crystalline phase and the lamellar structures of the PHB/PHB-HV blends forming the PHB-rich crystalline phase are slightly different from PHB-HV copolymers. The data on spherulite growth rate of these blends are, however, quite similar to those of the copolymers. The difference between the PHB/PHB-HV blends forming PHB-rich crystalline phase and PHB-HV copolymers is not so large.

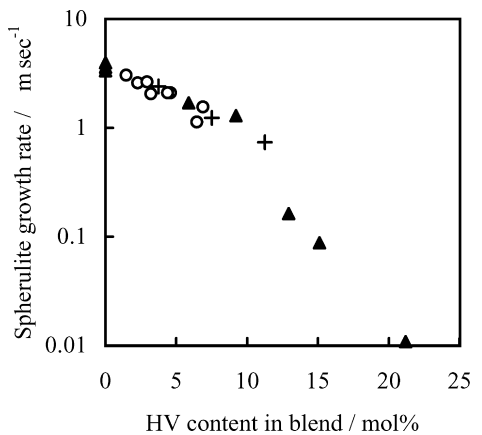

Fig. 9. Spherulite growth rate at 90 °C of PHB-HV copolymers (▲) and PHB/PHB-HV blends exhibiting complete-cocrystallization (○) and crystallization preferring PHB (+) as a function of overall HV content.

As shown in a previous paper [21], the crystalline phase structure of PHB-HV copolymers transforms from sandwich lamellae to uniform lamellae at ca. 10 mol% HV. In the uniform lamellar crystals, HV units are uniformly distributed. On the other hand, the sandwich lamellar crystals consist of edge parts and a core part between them: the core is composed entirely of HB units and HV units exist only in the edges. Because of the excess free energy of cocrystallization of HB and HV units, there must be a marked tendency for HV units to be excluded from the lamellae. In the PHB-HV copolymers with low HV content, the abundance of the long HB sequences strengthens this tendency to form the core. In this situation, HV units are probably concentrated on the surface of the core. Since the distortion of the crystalline lattice can be easily relaxed at the crystalline surface, these HV units can crystallize to form the edges with the HB units surrounding them. Therefore, the sandwich lamellae are considered to be a proper model for the isomorphism of PHB-HV with low HV content. The sandwich lamella is advantageous only when the average length of HB sequences is sufficiently large. So, the crystalline structure of PHB-HV copolymer transforms to uniform lamella at ca 10 mol% HV.

The driving forces behind the formation of the sandwich lamella in pure PHB-HV copolymers must also stimulate the cocrystallization in the blends of PHB and PHB-HV with low HV content. The long HB sequences of the copolymer, which would forms the core of the sandwich lamella in the pure state, must have marked tendency to cocrystallize with PHB to form the core of lamellae in the blends. Just like the case of pure copolymer, HV units are concentrated on the surface of cores to form the edges with the PHB chains surrounding them. Therefore, the sandwich lamella model may also well describe the lamellar structure of the blends of PHB and PHB-HV with low HV content.

4. Conclusion

By the comparison of the solid-state structures and crystallization kinetics between PHB-HV copolymers with narrow chemical compositional distribution and PHB/PHB-HV blends, the boundary between the PHB/PHB-HV blend that can be regarded as a simple PHB-HV and the one that must be treated as an exact blend are estimated. No difference was observed in structural parameters, melting behavior, and spherulite growth rate between the complete-cocrystallizable PHB/PHB-HV blends and the PHB-HV copolymers with the same overall HV content. Therefore, we can equate the structure of the complete-cocrystallizable blends with that of PHB-HV copolymers. On the other hand, the PHB/PHB-HV blends forming a PHB-rich crystalline phase has the amorphous layers thicker than that of the PHB-HV copolymers with the same overall HV content. The difference is, however, not so large and the other properties such as melting temperature and spherulite

growth rate are similar. Therefore, we can practically regard the blends forming a PHB-rich crystalline phase as a copolymer in some case. Needless to add, the PHB/PHB-HV blend forming more than two crystalline phases has to be treated as a exact blend.

The simplest method to identify the phase structure of PHB/PHB-HV blends and blends of two PHB-HV's is to measure the DSC melting curve and to compare the melting temperature of the blends with PHB-HV copolymers with narrow composition distribution. The melting temperature of such PHB-HV copolymers has been reported elsewhere [7]. Immiscible blends and blends forming more than two crystalline phases have two or more melting peaks. The blends forming complete cocrystals have only one melting peak at the temperature expected from the average HV content. If the melting temperature higher than the expectation, the crystalline phase rich in the component with higher crystallization rate is formed. This method may be applicable to the samples with broad chemical composition distribution and the sample with more complex composition distribution. If so, this method allows us to judge whether the PHB-HV sample as extracted from bacteria can be regarded as a simple copolymer.

Acknowledgements

The authors thank Prof. Asai of Tokyo Institute of Technology for his help with the WAXD and SAXS measurements. This work is partially supported by a Grant-in-Aid for Scientific Research on Priority Area, 'Sustainable Biodegradable Plastics', No.11217205 (2002) from the Ministry of Education, Science, Sports and Culture (Japan).

References

[1] Holmes PA. Phys Technol 1985;16:32.
[2] Doi Y, Tamaki A, Kunioka M, Soga K. Appl Microbiol Biotechnol 1988;28:330.
[3] Nakamura S, Kunioka M, Doi Y. Macromol Rep 1991;A28:15.
[4] Doi Y, Kitamura S, Abe H. Macromolecules 1995;28:4822–8.
[5] Kunioka M, Nakamura Y, Doi Y. Polym Commun 1988;29:174–6.
[6] Yoshie N, Inoue Y. Int J Biol Macromol 1999;25:193.
[7] Yoshie N, Menju H, Sato H, Inoue Y. Macromolecules 1995;28:6516.
[8] Yoshie N, Fujiwara M, Kasuya K, Abe H, Doi Y, Inoue Y. Macromol Chem Phys 1999;200:977.
[9] Cao A, Ichikawa M, Kasuya K, Yoshie N, Asakawa N, Inoue Y, Doi Y, Abe H. Polym J 1996;28:1096.
[10] Cao A, Ichikawa M, Ikejima T, Yoshie N, Inoue Y. Macromol Chem Phys 1997;198:3539.
[11] Watanabe T, He Y, Fukuchi T, Inoue Y. Macromol Biosci 2001;1:75.
[12] Ishida K, Wang Y, Inoue Y. Biomacromolecules 2001;2:1285.
[13] Yoshie N, Menju H, Sato H, Inoue Y. Polym J 1996;28:45.
[14] Saito M, Inoue Y, Yoshie N. Polymer 2001;42:5573.
[15] Yoshie N, Fujiwara M, Ohmori M, Inoue Y. Polymer 2001;42:8557.
[16] Na YH, Arai Y, Asakawa N, Yoshie N, Inoue Y. Macromolecules 2001;34:4834.
[17] Organ SJ, Barham PJ. Polymer 1993;34:459.
[18] Organ SJ. Polymer 1994;35:86.
[19] Pearce RP, Marchessault RH. Macromolecules 1994;27:3869.
[20] Doi Y, Kunioka M, Nakamura Y, Soga K. Macromolecules 1987;20:2988.
[21] Yoshie N, Saito M, Inoue Y. Macromolecules 2001;34:8953.
[22] Jimenez G, Asai S, Shishido A, Sumita M. Eur Polym J 2000;36:2039.
[23] Organ SJ, Barham PJ. Polymer 1993;34:2169.
[24] Bluhm TL, Hamer GK, Marchessault RH, Fyfe CA, Veregin RP. Macromolecules 1986;19:2871.
[25] Kamiya N, Sakurai M, Inoue Y, Chûjô R. Macromolecules 1991;24:2178.
[26] Kamiya N, Sakurai M, Inoue Y, Chûjô R. Macromolecules 1991;24:3888.
[27] Barker PA, Barham PJ, Martinez-Salazar J. Polymer 1997;38:913.
[28] VanderHart DL, Orts WJ, Marchessault RH. Macromolecules 1995;28:6394.